2010 IEEE International Conference on Robotics and Automation
Anchorage Convention District
May 3-8, 2010, Anchorage, Alaska, USA

Switching Control and Quick Stepping Motion Generation Based on the Maximal CPI Sets for Falling Avoidance of Humanoid Robots

Ko Yamamoto and Yoshihiko Nakamura

Abstract— **Humanoid robots should be able to stand and walk in the presence of external disturbances. This paper addresses the robustness of a humanoid robot to unknown disturbances. Applying the maximal CPI set, it becomes possible to consider the physical constraint explicitly in the COG-ZMP inverted pendulum model control. In our previous research, the convergence speed of COG was improved by applying the switching control based on the maximal CPI set to the stabilization control assuming the contact region is constant. This paper presents updating calculation method of the maximal CPI set when the contact region changes, and the authors propose a falling avoidance control as an application of it. Detecting the stepping necessity based on the maximal CPI set enables to unify the upright position stabilization and stepping motion for falling avoidance. The validity of the proposed method is verified with experiments.**

I. Introduction

In real environments and situations, unknown disturbances act on humanoid robots. For a humanoid robot to work in the human life environments, an issue to be solved is the realization of reliable and robust stabilizing controllers. For balancing control, some researchers proposed to compensate errors of the Zero Moment Point (ZMP) [1], which is defined as the centroid of the reaction force. Sano and Furusho [2] and Kajita et al. [3] proposed a compensation method of the ZMP errors by the ankle torque. Hirai et al. [4] and Nagasaka [5] proposed to set the body motion compliance and to compensate the ZMP errors. On the other hand, another approach considers the ZMP as control input and the center of gravity (COG) of the robot as controlled variable [6][7]. Assuming the mass concentrated model of the biped locomotion system, its dynamics is equivalent to that of the inverted pendulum whose support point is the ZMP and the tip is the COG. By abstracting this macroscopic dynamics, the computation cost becomes low compared with the other control methods using the strict dynamics [8]. Mitobe et al. [6] proposed a method to determine the ZMP using the control law of the inverted pendulum. Sugihara and Nakamura [7] proposed to determine the ZMP based on PID control of the inverted pendulum.

However, the base link of the biped locomotion system is not fixed to the environments and there exists the physical constraint on the ZMP. In previous research, this constraint is not considered in the control law of the COG-ZMP inverted pendulum model. In some cases, it is impossible to realize the ZMP motion which is requested by the control law. It is necessary to consider the physical constraint explicitly. The authors [9] proposed to apply the maximal Constraint Positively Invariant (CPI) set [10] to control of the COG-ZMP inverted pendulum model. The convergence speed of COG was improved by applying the switching control [11] based on the maximal CPI set. However, we assumed the stabilization in the upright position on the constant contact region. When the contact region changes after stepping motion, we have to update the maximal CPI set.

In this paper, the authors propose a updating method of the maximal CPI set. Whereas the original calculation method consists of the iteration of the linear programming and requires offline computation, the proposed method enables on-line computation. We also propose a falling avoidance control method. The stepping necessity is detected based on the maximal CPI set, which unifies the upright position stabilization and stepping motion for falling avoidance. Firstly, we explain the COG-ZMP inverted pendulum control in Sect. II, and overview the switching control based on the maximal CPI set in Sect. III. Sect. IV presents updating method of the maximal CPI set when the contact region changes. In Sect. V, we present falling avoidance control and shows some examples of stepping motion for falling avoidance. Sect. VI, reports experimental results, and verifies the validity of the proposed method. Sect. VII concludes and summarizes this paper.

II. COG-ZMP Inverted Pendulum Model Control

Assuming the mass concentrated model of humanoid robots, its motion equations are formulated as follows:

$$\ddot{x}_G = \omega_G^2(x_G - x_Z) \tag{1}$$

$$\ddot{y}_G = \omega_G^2(y_G - y_Z) \tag{2}$$

$$\ddot{z}_G = \frac{f_z}{m} - g \tag{3}$$

where the COG of the robot is $\boldsymbol{p}_G = [x_G\ y_G\ z_G]^T$, the ZMP is $\boldsymbol{p}_Z = [x_Z\ y_Z\ z_Z]^T$, the total mass is m, and vertical external force is f_z. And, ω_G is defined by $\omega_G^2 \equiv (\ddot{z}_G + g)/(z_G - z_Z)$. When vertical motion is small, we can regard ω_G as constant value.

Equation (1) and (2) are equivalent to the dynamics of the inverted pendulum whose support point is the ZMP and tip is the COG, as shown in Fig. 1. From this point of view, there are researches to control the COG regarding the ZMP as control input [6][7]. However, there exists the following

This research is partly supported by Special Coordination Funds for Promoting Science and Technology, IRT Foundation to Support Man and Aging Society.

K. Yamamoto is with the Department of Mechanical Science and Engineering, Tokyo TECH, 2-12-1 Oookayama, Megutro-ku, 152-8552 Tokyo, Japan yamamoto@micro.mep.titech.ac.jp

Y. Nakamura is with the Department of Mechano-Informatics, University of Tokyo, 7-3-1 Hongo, Bunkyo-ku, 113-8656 Tokyo, Japan

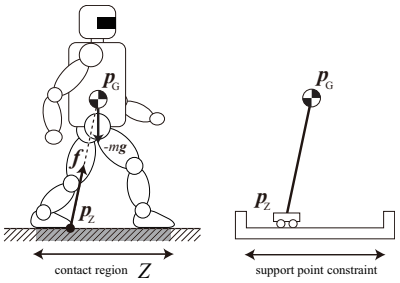

Fig. 1. Mass concentrated model of humanoid robot (left) and inverted pendulum model with support point constrained (right)

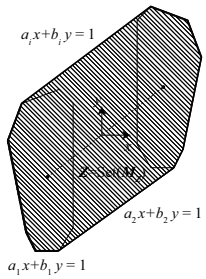

Fig. 2. Contact region approximated by a convex hull

physical constraint on the ZMP because the biped locomotion system has no link fixed to the environment.

$$\boldsymbol{p}_Z \in Z \tag{4}$$

where Z is the contact region of the robot. Therefore, when a large disturbance acts on the robot, the ZMP reaches the edge of the contact region and the robot falls over the edge. Hence, the controller is required to consider this constraint explicitly.

III. Switching Control Based on the Maximal CPI set for Humanoid Robots [9]

A. Formulation of Linear Discrete-time System

In order to consider constraints in the system explicitly, the maximal CPI set has been proposed [10]. The authors [9] proposed to apply the maximal CPI set and switching control based on it to the COG-ZMP inverted pendulum control. Firstly, we convert the motion equations (1)-(2) to a linear discrete-time system in order to introduce the maximal CPI set. Let us choose the COG x_G, its velocity $\dot{x}_G$ and the ZMP x_Z as the state variable, and the differential of the ZMP as the control input.

$$\boldsymbol{x} \equiv \begin{bmatrix} x_G & \dot{x}_G & x_Z & y_G & \dot{y}_G & y_Z \end{bmatrix}^T \tag{5}$$

$$\boldsymbol{u} \equiv \begin{bmatrix} \dot{x}_Z & \dot{y}_Z \end{bmatrix}^T \tag{6}$$

We include the ZMP in the state variable in order to consider the physical constraint. Then, we convert (1) and (2) to the following linear system.

$$\dot{\boldsymbol{x}} = \boldsymbol{A}_C \boldsymbol{x} + \boldsymbol{B}_C \boldsymbol{u} \tag{7}$$

$$\boldsymbol{A}_C \equiv \begin{bmatrix} 0 & 1 & 0 & & & \\ \omega_G^2 & 0 & -\omega_G^2 & & \boldsymbol{O} & \\ 0 & 0 & 0 & & & \\ & & & 0 & 1 & 0 \\ & \boldsymbol{O} & & \omega_G^2 & 0 & -\omega_G^2 \\ & & & 0 & 0 & 0 \end{bmatrix} \tag{8}$$

$$\boldsymbol{B}_C \equiv \begin{bmatrix} 0 & 0 & 1 & & \boldsymbol{o} & \\ & \boldsymbol{o} & & 0 & 0 & 1 \end{bmatrix}^T \tag{9}$$

Discretizing (7), we get the following linear discrete-time system.

$$\boldsymbol{x}(t+1) = \boldsymbol{A}\boldsymbol{x}(t) + \boldsymbol{B}u(t) \tag{10}$$

Let us consider that the input $\boldsymbol{u}$ is determined by the following state feedback $\boldsymbol{F}$, it is

$$\boldsymbol{u} = -\boldsymbol{F}\boldsymbol{x} \tag{11}$$

where the main focus of the control is set as the regulation of the COG to the origin. In this respect, we set the origin of the controller coordinate to be the center point of both feet. It is possible to design the state feedback gain $\boldsymbol{F}$ by using the pole assignment or the optimum regulator, for example. Note that on-diagonal elements of the gain matrix $\boldsymbol{F}$ become zero because on-diagonal elements of $\boldsymbol{A}_C$ and $\boldsymbol{B}_C$ are also zero.

$$\boldsymbol{F} = \begin{bmatrix} \boldsymbol{f}_x^T & \boldsymbol{0} \\ \boldsymbol{0} & \boldsymbol{f}_y^T \end{bmatrix}, \quad \boldsymbol{f}_x, \boldsymbol{f}_y \in \boldsymbol{R}^3 \tag{12}$$

Substituting (11) to (10), we get the following closed loop Σ.

$$\boldsymbol{x}(t+1) = \tilde{\boldsymbol{A}}\boldsymbol{x}(t), \quad \tilde{\boldsymbol{A}} \equiv \boldsymbol{A} - \boldsymbol{B}\boldsymbol{F} \tag{13}$$

From (8), (9) and (13), off-diagonal elements of $\tilde{\boldsymbol{A}}$ also become zero. This result implies that it is possible to design the compensator in x and y directions independently.

B. Formulation of Contact Region and Physical Constraint

We define a vector specifying the ZMP: $\boldsymbol{z} \equiv \begin{bmatrix} x_Z & y_Z \end{bmatrix}^T$. The relationship between a state vector $\boldsymbol{x}$ and $\boldsymbol{z}$ is represented by the following equation.

$$\boldsymbol{z}(t) = \boldsymbol{C}\boldsymbol{x}(t), \quad \boldsymbol{C} \equiv \begin{bmatrix} 0 & 0 & 1 & 0 & 0 & 0 \\ 0 & 0 & 0 & 0 & 0 & 1 \end{bmatrix} \tag{14}$$

In this paper, we assume that the contact region is represented by a convex hull. In this assumption, the contact region Z is represented by the convex polyhedron delimiting the set

$$Z \equiv \left\{ \boldsymbol{z} \in \boldsymbol{R}^2 \mid \boldsymbol{M}_Z \boldsymbol{z} \leq \boldsymbol{1} \right\} \tag{15}$$

where $\boldsymbol{M}_Z \in \boldsymbol{R}^{p \times 2}$ is a matrix specifying the convex polyhedron. p is the number of the edges of the polyhedron. $\boldsymbol{1}$ is the vector with all elements set to 1, and the inequality sign applies to each row element in (15). In following discussion, we call the matrix $\boldsymbol{M}_Z$ as the *constraint matrix* of the set $Z \equiv \mathrm{Set}(\boldsymbol{M}_z)$.

As an example, let us consider a simple case when the contact region is given as follows:

$$x_{\min} \leq x_Z \leq x_{\max}, \quad y_{\min} \leq y_Z \leq y_{\max} \tag{16}$$

In this case, the constraint matrix is equal to

$$\boldsymbol{M}_{Z0} = \begin{bmatrix} \frac{1}{x_{\min}} & 0 \\ \frac{1}{x_{\max}} & 0 \\ 0 & \frac{1}{y_{\min}} \\ 0 & \frac{1}{y_{\max}} \end{bmatrix} \tag{17}$$

Therefore, we can represent the physical constraint of the ZMP as follows:

$$\boldsymbol{z}(t) \in Z \tag{18}$$

C. Maximal CPI set

Under the assumption that 1) $\tilde{\boldsymbol{A}}$ is asymptotically stable and 2) Z includes the origin, the maximal CPI set O_∞ of a closed-loop (13) is defined as follows [10]: *The set of all possible initial state in which it is guaranteed that the state converges to the origin point without breaking the constraint.* The maximal CPI set is calculated as a convex polyhedron as follows:

$$O_\infty = \left\{ \boldsymbol{x} \in \boldsymbol{R}^6 \mid \boldsymbol{S}_{\max} \boldsymbol{x} \leq \boldsymbol{1} \right\} \tag{19}$$

where $\boldsymbol{S}_{\max}$ is a matrix specifying the maximal CPI set. According to [10], it is possible to compute $\boldsymbol{S}_{\max}$ by the finite number of iterations of the linear programming as follows:

1) Calculate a matrix $\boldsymbol{S}_0$ as follows:

$$\boldsymbol{S}_0 = \boldsymbol{M}_Z \boldsymbol{C} \tag{20}$$

2) In the i-th step, we formulate $\boldsymbol{S}_i$ as follows:

$$\boldsymbol{S}_i = \begin{bmatrix} \boldsymbol{S}_0 \\ \boldsymbol{S}_{i-1} \tilde{\boldsymbol{A}} \end{bmatrix} \tag{21}$$

3) If $\mathrm{Set}(\boldsymbol{S}_i) = \mathrm{Set}(\boldsymbol{S}_{i-1})$, the procedure ends and the matrix $\boldsymbol{S}_{\max}$ specifying the maximal CPI set is obtained as $\boldsymbol{S}_{\max} = \boldsymbol{S}_i$. Otherwise, increment i and return to the 2).

As a result, we obtain $\boldsymbol{S}_{\max}$ as the following form.

$$\boldsymbol{S}_{\max}(\boldsymbol{M}_Z) = \begin{bmatrix} \boldsymbol{M}_Z & \boldsymbol{O} & \dots & \boldsymbol{O} \\ \boldsymbol{O} & \boldsymbol{M}_Z & \dots & \boldsymbol{O} \\ \vdots & \vdots & \ddots & \vdots \\ \boldsymbol{O} & \boldsymbol{O} & \dots & \boldsymbol{M}_Z \end{bmatrix} \begin{bmatrix} \boldsymbol{C} \\ \boldsymbol{C}\tilde{\boldsymbol{A}} \\ \vdots \\ \boldsymbol{C}\tilde{\boldsymbol{A}}^k \end{bmatrix} \tag{22}$$

where k is the number of the iterations.

D. Switching Control Based on the Maximal CPI Set

In general, the maximal CPI set becomes small when $\boldsymbol{F}$ with a high convergence speed is applied. On the other hand, the maximal CPI set becomes large when $\boldsymbol{F}$ with a low convergence speed is applied. Using this property, the switching control[11] has been proposed.

Suppose that the state feedback gains $\boldsymbol{F}_i, (i = 1, \dots, k)$ are designed so that each maximal CPI set O_∞^i satisfies the inclusion relation, $O_\infty^k \subset \cdots \subset O_\infty^1$, as shown in the left side of Fig. 3. In other words, the sets O_∞^i are ordered according to the convergence speed achieved with corresponding $\boldsymbol{F}_i$. In the switching control, the performance is improved by choosing maximum index i that satisfies $\boldsymbol{x}(t) \in O_\infty^i$. The right side of Fig. 3 shows the block diagram of the switching control. A *supervisor* switches the feedback gain $\boldsymbol{F}_i$ depending on which O_∞^i includes the current state.

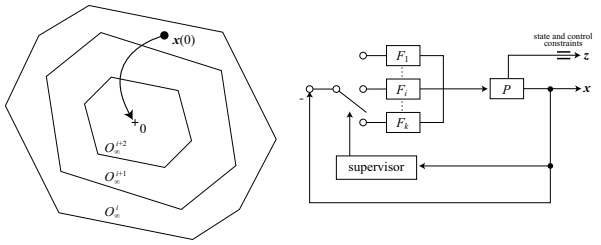

Fig. 3. Inclusion relationship of the maximal CPI sets (left) and block diagram of switching control (right). *Supervisor* switches the compensator $\boldsymbol{F}_i$ and outputs the current state as the initial state of Σ_i.

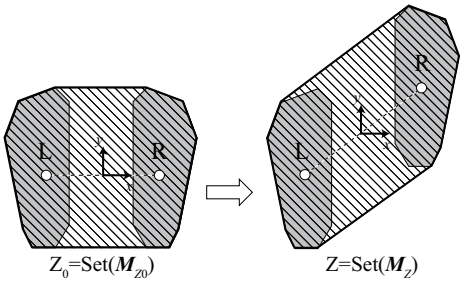

Fig. 4. Example of contact region change when the robot steps the right foot forward. After the foot landing, the control coordinate is reset as its origin is located at the center point of both feet.

In the stabilization in the upright position of humanoid robots, the convergence speed of the COG is improved by applying the switching control.

IV. Maximal CPI set in Changing Contact Region

In the biped locomotion, the contact region often changes discontinuously. Therefore, it is necessary to update the maximal CPI set in real time. In this section, we explain updating method of the maximal CPI set without iteration of the linear programming.

Suppose that the initial contact region is specified by $Z_0 = \mathrm{Set}(\boldsymbol{M}_{Z0})$ as shown in the left side of Fig. 4, and that the maximal CPI set matrix $\boldsymbol{S}_{\max}(\boldsymbol{M}_{Z0})$ is calculated in advance. From (22), $\boldsymbol{S}_{\max}(\boldsymbol{M}_{Z0})$ is represented by the following.

$$\boldsymbol{S}_{\max}(\boldsymbol{M}_{Z0}) = \begin{bmatrix} \boldsymbol{M}_{Z0} & \boldsymbol{O} & \dots & \boldsymbol{O} \\ \boldsymbol{O} & \boldsymbol{M}_{Z0} & \dots & \boldsymbol{O} \\ \vdots & \vdots & \ddots & \vdots \\ \boldsymbol{O} & \boldsymbol{O} & \dots & \boldsymbol{M}_{Z0} \end{bmatrix} \boldsymbol{\Phi} \tag{23}$$

$$\boldsymbol{\Phi} \equiv \begin{bmatrix} \boldsymbol{C}^T & (\boldsymbol{C}\tilde{\boldsymbol{A}})^T & \dots & (\boldsymbol{C}\tilde{\boldsymbol{A}}^k)^T \end{bmatrix}^T \tag{24}$$

Consider that the contact region changes to $Z = \mathrm{Set}(\boldsymbol{M}_Z)$ after the foot landing as shown in the right side of Fig. 4. Because the matrix $\boldsymbol{\Phi}$ has been already calculated, we can

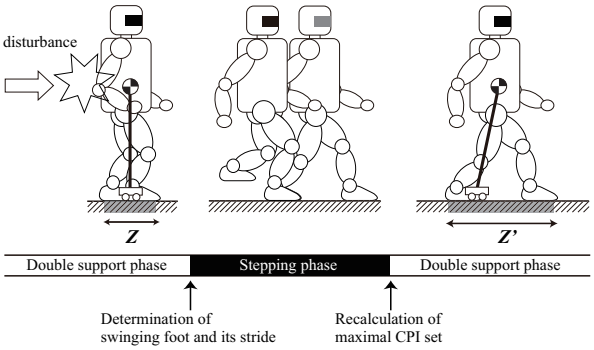

Fig. 5. Sequence of falling avoidance control

compute $\boldsymbol{S}_{\max}(\boldsymbol{M}_Z)$ online as follows:

$$\boldsymbol{S}_{\max}(\boldsymbol{M}_Z) = \begin{bmatrix} \boldsymbol{M}_Z & \boldsymbol{O} & \dots & \boldsymbol{O} \\ \boldsymbol{O} & \boldsymbol{M}_Z & \dots & \boldsymbol{O} \\ \vdots & \vdots & \ddots & \vdots \\ \boldsymbol{O} & \boldsymbol{O} & \dots & \boldsymbol{M}_Z \end{bmatrix} \boldsymbol{\Phi} \tag{25}$$

V. Application to Falling Avoidance Control

A. Stepping Necessity Detection based on Maximal CPI Set

If a disturbance to the robot becomes so large that the system requires the response with the ZMP constraint violated, ZMP becomes located in the edge of support region and the robot is about to fall. In order to avoid falling, it is necessary for the robot to step and enlarge the support region actively. In particular, it is necessary to detect falling in the future because the robot must switch the strategies and generate stepping motion before he falls completely.

In this respect, we propose falling detection based on the maximal CPI set: When the current state $\boldsymbol{x}(t)$ is not included in the maximal CPI set O_∞ due to disturbance, we determine the necessity to step.

$$\boldsymbol{x}(t) \notin O^i_\infty \quad (i = 1, \dots, k) \tag{26}$$

Using the maximal set as an indicator for switching the strategies, it is possible to unify generation of stepping motion and COG control after foot landing.

Using the stepping necessity detection, we propose a falling avoidance control method. Fig. 5 shows proposed control sequence. As the stepping necessity is detected, a stepping motion is generated with the Boundary Condition Relaxation method [12], which is appropriate in the following respects: 1) It is possible to plan the referential trajectory of one step motion in real time. 2) It is suitable to plan a quick legged motion because reference ZMP is designed with an exponential function. After the foot landing, we recalculate the maximal CPI set as mentioned in the previous section, and the switching control is applied again.

In the following section, we explain how to determine desired swinging foot position.

B. Determination of Swinging Foot and its Stride

Firstly, we set coordinate Σ_i fixed to the foot $i = L, R$, whose origin is the center point of foot sole and orientation coincide with one of the control coordinate Σ_C, as shown in left side of Fig. 6. In the coordinate Σ_R, we set motion range of the right foot D_L by a semi-ellipsoid assuming the left foot is fixed.

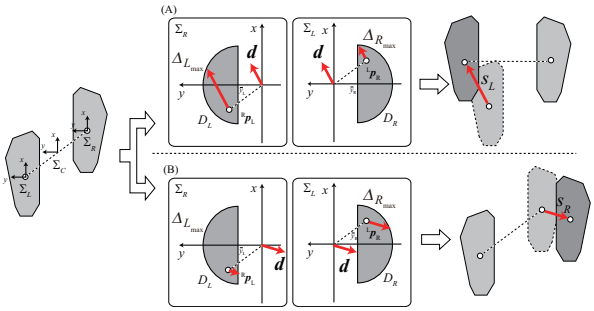

Fig. 6. Examples to determine swinging foot

$$D_L = \left\{ x, y \mid y \geq \bar{y}_L \ \cap \ \frac{x^2}{a^2} + \frac{(y - \bar{y}_L)^2}{b^2} \leq 1 \right\} \tag{27}$$

In a similar way, we set motion range of the left foot D_R in the coordinate Σ_L assuming the right foot is fixed

$$D_R = \left\{ x, y \mid y \leq \bar{y}_R \ \cap \ \frac{x^2}{a^2} + \frac{(y - \bar{y}_R)^2}{b^2} \leq 1 \right\} \tag{28}$$

When ZMP error $\Delta \boldsymbol{p}_Z$ is caused by the disturbance, the swinging foot is determined by the following procedure.

1) compute the disturbance direction vector as $\boldsymbol{d} \equiv \Delta \boldsymbol{p}_Z / \|\Delta \boldsymbol{p}_Z\|$.
2) in the coordinate Σ_R, calculate a vector extended from ${}^R\boldsymbol{p}_L$ to the border line of D_L, and put the vector $\Delta_{L\max}$.
3) $\Delta_{R\max}$ is also calculated in the coordinate Σ_L.
4) if $\|\Delta_{L\max}\| \geq \|\Delta_{R\max}\|$, the left foot is chosen as swinging foot. Otherwise, the right foot is chosen.

When $\boldsymbol{d}$ is given by the arrow shown in (A) of Fig. 6, $\|\Delta_{L\max}\| \geq \|\Delta_{R\max}\|$ and the left foot is chosen. On the other hand, when $\boldsymbol{d}$ is given by the arrow shown in (B), $\|\Delta_{L\max}\| < \|\Delta_{R\max}\|$ the right foot is chosen.

Then, we calculate the stride of step as follows:

$$s_i = \begin{cases} \alpha \|\Delta \boldsymbol{p}_Z\| & (\text{if} \quad \alpha \|\Delta \boldsymbol{p}_Z\| < \|\Delta_{i\max}\|) \\ \|\Delta_{i\max}\| & (\text{if} \quad \alpha \|\Delta \boldsymbol{p}_Z\| \geq \|\Delta_{i\max}\|) \end{cases} \tag{29}$$

α is the coefficient which means ratio of stride to ZMP error and determined experimentally.

C. Examples of Stepping Motion Generation

We simulated stepping motion generation for falling avoidance when several disturbances were imposed. We assumed a miniature humanoid robot, UT-μ2 [13]. Fig. 7 shows the external view and joint configuration of UT-μ2.

Firstly, we set ZMP error to be $\Delta \boldsymbol{p}_Z = [-0.03 \ 0 \ 0]^T$ assuming that a disturbance imposed backward. Fig. 8(a) shows snapshots of the resultant whole body motion by solving inverse kinematics. The stepping necessity was detected and a backward stepping motion was generated automatically.

Next, we set ZMP error to be $\Delta \boldsymbol{p}_Z = [0.03 \ 0.685 \ 0]^T$ assuming that a disturbance imposed from diagonally forward left. Fig. 8(b) shows snapshots of the resultant whole body

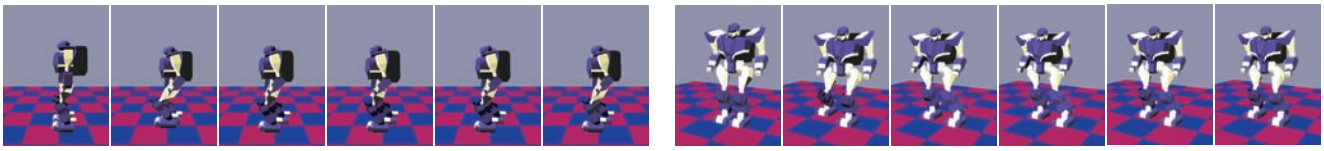

(a) (b)

Fig. 8. Snapshots of the resultant whole body motion by when disturbances were imposed from backward (a) and diagonally forward left (b).

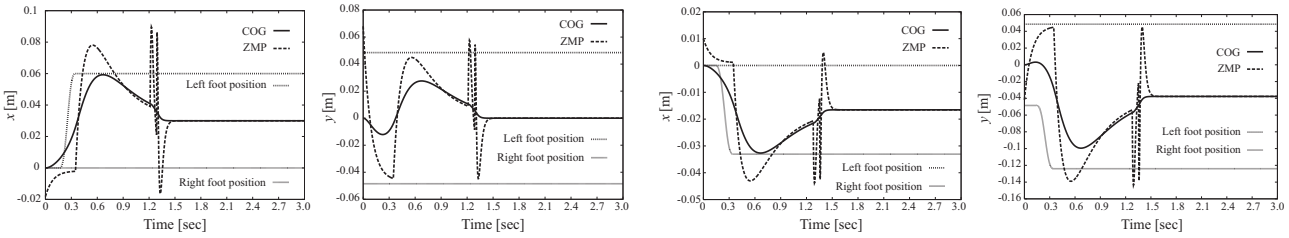

(a) (b)

Fig. 9. Response of COG and ZMP assuming that a disturbance imposed from backward (a) and diagonally forward left (b).

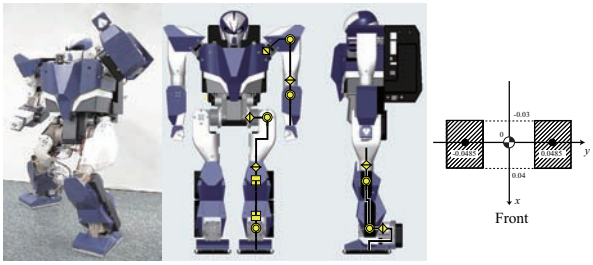

Main specification

Height : 54[mm]
Weight : 8.0[kg]
Number of joints : 20 (4 at each arms, 6 at each legs)

Fig. 7. External view and joint configuration of UT-μ2:magnum, and the initial foot placement in simulations and experiments

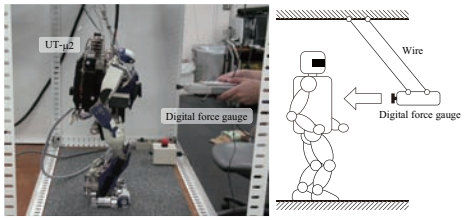

Fig. 10. Experimental setup for the switching control when a disturbance is imposed on the robot.

motion. The right foot was chosen as swinging foot based on proposed determination algorithm.

Fig. 9(a) and Fig. 9(b) show the response of COG, ZMP and left and right foot position. It is apparent that the state is controlled by the switching control after foot landing.

VI. Experiment

A. Experimental Setup

We implemented the proposed control method on UT-μ2. In order to evaluate the robot response to imposed disturbance, we set up an experimental apparatus as shown in Fig. 10. A digital force gauge, Z2-500N (IMADA), was used for imposing the disturbance to the robot. We hanged it from the ceiling with two wires, and enabled it to impose the horizontal disturbance as precisely as possible.

Fig. 11 shows total block diagram of proposed falling avoidance control. The switching controller or stepping motion generator outputs desired COG position ${}^d\boldsymbol{p}_G$. In "COG control" block, desired joint angle vector ${}^d\boldsymbol{\theta}$ is obtained from ${}^d\boldsymbol{p}_G$ by solving the inverse kinematics with COG Jacobian [14]. "COG reference shaping" compensates the gravity effect by feedback of the actual COG [9]. We also apply Kalman Filter in order to filter out the noise of sensors.

B. Experimental Results

Fig. 12 and 13 are snapshots of the robot response. In the case of Fig. 12, a disturbance was imposed from backward and the robot steps forward. The right foot is chosen as swinging foot. It is verified that the robot steps in the appropriate direction depending on the disturbance direction. After the foot landing, it took about 0.15 ms to update the maximal CPI set.

In the case of Fig. 13, disturbance was imposed from diagonally forward left and the right foot is chosen as swinging foot in a similar way to the simulation. From the pictures, however, it was seen that the robot rotated around the yaw axis, slightly. This was because ZMP was not manipulated as planned, especially in y-axis.

Fig. 14 shows measured COG, ZMP and left and right foot position during experiments.

VII. Conclusion

We proposed the on-line updating method of the maximal CPI set when the contact region changing. The falling avoidance control method was also proposed based on the set. By detecting the stepping necessity using the maximal CPI set, the upright position stabilization and stepping motion for falling avoidance are unified. The validity was verified in the experiments.

In this paper, compensation or stabilizing control were not discussed during the stepping motion. In particular, modeling errors became a problem in the experiments. In particular, it is considered that main causes are modeling error of inertia

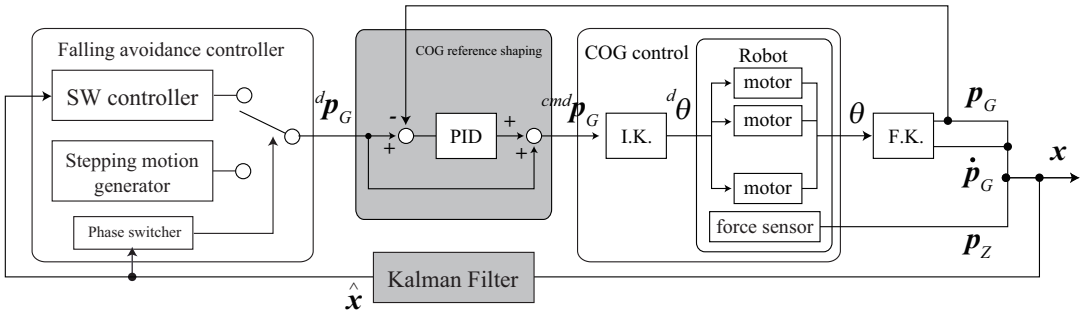

Fig. 11. Total block diagram of proposed falling avoidance control

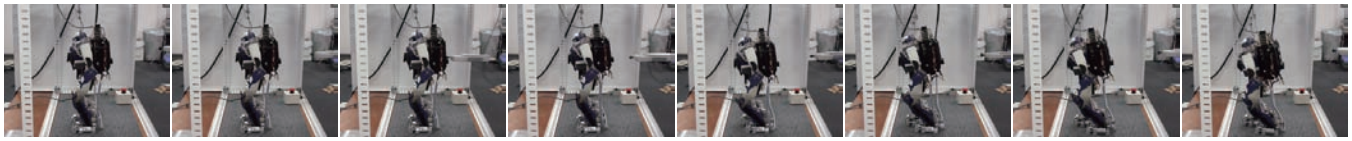

Fig. 12. Snapshots of the robot response when the disturbance was imposed from backward. The stepping necessity was detected and the robot stepped forward.

Fig. 13. Snapshots of the robot response when a disturbance was imposed from diagonally forward left. The stepping necessity was detected and the robot stepped diagonally backward right.

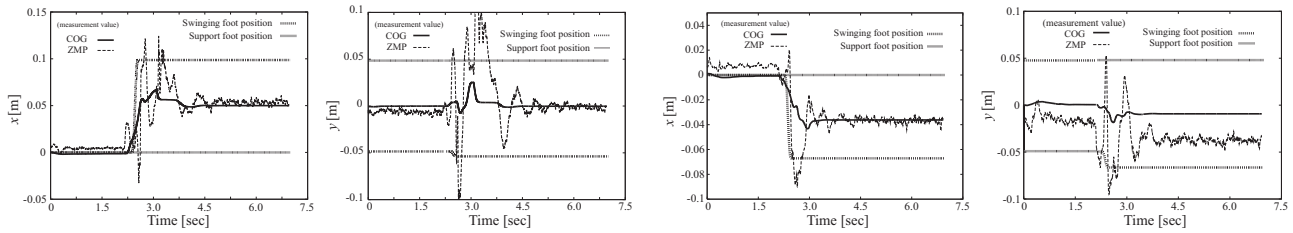

(a) (b)

Fig. 14. Response of COG and ZMP when disturbances were imposed from backward (a) and diagonally forward left (b).

parameters and moment around COG. In future works, it is necessary to compensate these modelling errors.

REFERENCES

[1] M. Vukobratović and J. Stepanenko., "On the Stability of Anthropomorphic Systems." *Mathematical Biosciences*, vol. 15, pp. 1–37, 1972.

[2] J. Furusho and A. Sano, "Sensor-based control of a nine-link biped," *International Journal of Robotics Research*, vol. 9, no. 2, pp. 83–98, 1990.

[3] S. Kajita *et al.*, "Balancing a Humanoid Robot Using Backdrive Concerned Torque Control and Direct Angular Momentum Feedback," in *Proceedings of the 2001 IEEE International Conference on Robotics and Automation (ICRA2001)*, 2001, pp. 3376–3382.

[4] K. Hirai., "Current and Future Perspective of Honda Humanoid Robot." in *Proceedings of the 1997 IEEE/RSJ International Conference on Intelligent Robots and Systems*, 1997., pp. 500–508.

[5] K. Nagasaka *et al.*, "Stabilization of dynamic walk on a humanoid using torso position compliance control (in japanese)," in *Proceedings of the 17th Annual Conference of the Robotics Society in Japan*, 1999, pp. 1193–1194.

[6] K. Mitobe, G. Capi, and Y. Nasu, "Control of walking robots based on manipulation of the zero moment point," *Robotica*, vol. 18, pp. 651–657, 2000.

[7] T. Sugihara, Y. Nakamura, and H. Inoue, "Realtime Humanoid Motion Generation through ZMP Manipulation based on Inverted Pendulum Control," in *Proceedings of the 2002 IEEE International Conference on Robotics and Automation*, 2002, pp. 1404–1409.

[8] Y. Fujimoto and A. Kawamura, "Simulation of an Autonomous Biped Walking Robot Including Enviromental Force Interaction," *IEEE Robotics and Automation Magazine*, 1998.

[9] K. Yamamoto and Y. Nakamura, "Switching Feedback Controllers Based on the Maximal CPI Sets for Stabilization of Humanoid Robot," in *Proceedings of 2009 IEEE/RAS International Conference on Humanoid Robots (Humanoids2009)*, 2009, pp. 549–554.

[10] E. G. Gilbert and K. T. Tan, "Linear Systems with State and COntrol Constraints: The Theory and Application of Maximal Output Admmisible Sets," *IEEE Transaction on Automatic Control*, vol. 36, no. 9, pp. 1008–1020, 1991.

[11] K. Hirata and M. Fujita, "Observer Based Switching Control for Systems with State and Control Constraints," in *Proceedings of the American Control Conference*, 2001, pp. 1892–1897.

[12] T. Sugihara and Y. Nakamura, "A Fast Online Gait Planning with Boundary Condition Relaxation for Humanoid Robots," in *Proceedings of the 2005 IEEE International Conference on Robotics and Automation*, 2005, pp. 306–311.

[13] T. Sugihara, K. Yamamoto, and Y. Nakamura., "Hardware design of high performance miniature anthropomorphic robots." *Robotics and Autonomous System*, vol. 56, Issue 1, pp. 82–94, 2007.

[14] T. Sugihara and Y. Nakamura, "Whole-body Cooperative Balancing of Humanoid Robot using COG Jacobian," in *Proceedings of the 2002 IEEE/RSJ International Conference on Intelligent Robots and Systems (IROS2002)*, 2002, pp. 2575–2580.